Supporting Information

Structure and Sodium Channel Activity of an Excitatory I_1-Superfamily Conotoxin [†]

Olga Buczek[‡§], Daxiu Wei[‖§], Jeffrey J. Babon[‖], Xiaodong Yang[‖], Brian Fiedler[‡], Ping Chen[‡], Doju Yoshikami[‡], Baldomero M. Olivera[‡], Grzegorz Bulaj[¶], and Raymond S. Norton[‖ *]

Department of Biology, University of Utah, Salt Lake City, Utah, 84112, USA, The Walter and Eliza Hall Institute of Medical Research, 1G Royal Parade, Parkville 3050 Australia, and Department of Medicinal Chemistry, University of Utah, Salt Lake City, Utah, 84108, USA

Running title: *Structure and Na channel activity of an excitatory conotoxin*

[*] This work was supported in part by N.I.H. grant GM 48677 (to B.M.O.), from the National Institute of General Medical Sciences. R.S.N. acknowledges support from the NHMRC.

[§] These authors contributed equally to this work.

[*] To whom correspondence should be addressed: Raymond S. Norton, The Walter & Eliza Hall Institute of Medical Research, 1G Royal Parade, Parkville, 3050, Australia. Email: ray.norton@wehi.edu.au Phone: +61 3 9345 2306. Fax: +61 3 9345 2686.

[‡] University of Utah, Department of Biology

[‖] The Walter and Eliza Hall Institute of Medical Research

[¶] University of Utah, Department of Medicinal Chemistry

Supporting Information consists of 3 TABLES and 5 FIGURES

Table S1. Chemical shifts and $^{3}J_{HNHA}$ of ι-RXIA[L-Phe44] in 95% H_2O/5% $^{2}H_2O$ at pH 5.9 and 298 K. Where there is no entry for $^{3}J_{HNHA}$, the peak intensity was weak in the DQF-COSY spectrum and the derived coupling constant was not reliable.
Backbone amide exchange rates are indicated as follows: residue names in **bold** were visible in a TOCSY started soon after dissolution of the peptide in $^{2}H_2O$ at pH 5.5 and 278 K, and in 1D spectra at the conclusion of the TOCSY (3 h acquisition), those underlined were visible in 1D spectra recorded before the TOCSY but not after. Residues not shown underlined or in bold exchanged too quickly with $^{2}H_2O$ for the peaks to be observed in a 1D proton spectrum.

Residue	HN	$C^{\alpha}H$	$C^{\beta}H$	C^{α}	Other	$^{3}J_{HNH\alpha}$
Gly1	--	4.02, 3.93		43.5		--
Hyp2	--	4.50	2.04, 1.99	60.8	$C^{\gamma}H$ 4.63 $C^{\delta}H_2$ 3.80	--
Ser3	8.56	4.39	3.80	58.7		7.9
Phe4	8.22	4.73	3.17, 3.02	57.5	C(2,6)H 7.26 C(3,5)H 7.36	7.5
Cys5	7.99	4.51	3.04, 2.80	54.3		6.8
Lys6	8.74	4.34	2.16, 1.75	57.4	$C^{\gamma}H$ 1.58, 1.48 $C^{\delta}H_2$ 1.60 $C^{\varepsilon}H_2$ 3.07	6.1
Ala7	8.42	4.09	1.44	51.4		7.1
Asp8	8.17	4.10	2.74, 2.55	55.7		7.6
Glu9	9.21	3.80	2.29, 2.23	58.2	$C^{\gamma}H_2$ 2.60	
Lys10	7.50	4.70	2.04, 1.76	53.7	$C^{\gamma}H$ 1.57, 1.48 $C^{\delta}H_2$ 1.69 $C^{\varepsilon}H_2$ 3.04	6.7
Hyp11	--	4.62	2.39, 2.00	61.1	$C^{\gamma}H$ 5.18 $C^{\delta}H_2$ 3.90, 3.80	--
Cys12	8.29	4.81	3.17, 3.10	54.4		7.5
Glu13	8.79	4.16	1.63, 1.44	57.1	$C^{\gamma}H_2$ 1.95, 1.77	7.9
Tyr14	7.91	4.82	3.39, 2.55	55.5	C(2,6)H 7.21 C(3,5)H 6.81	7.8
His15	8.50	4.51	3.07	57.1	C(2)H 7.78 C(4)H 7.13	
Ala16	8.32	4.24	1.45	54.1		7.9
Asp17	7.88	4.45	3.20, 2.70	55.2		7.7
Cys18	8.08	4.92	3.16, 2.56	54.0		9.6
Cys19	9.21	4.51	3.14, 2.59	54.3		7.3
Asn20	8.58	5.03	2.78, 2.42	53.2	$N^{\gamma}H_2$ 9.13, 6.76	10.6
Cys21	8.12	5.25	3.09, 2.65	53.0		9.5
Cys22	12.10	5.08	2.79, 2.56	55.8		
Leu23	8.75	4.71	1.62, 1.54	57.5	$C^{\gamma}H$ 1.48 $C^{\delta}H_3$ 1.07, 0.82	10.4

Residue	HN	$C^{\alpha}H$	$C^{\beta}H$	C^{α}	Other	$^{3}J_{HNH\alpha}$
Ser24	8.92	3.88	4.09, 3.83	58.3		8.7
Gly25	7.61	4.09, 3.80		45.7		--
Ile26	7.53	4.72	1.62	59.3	$C^{\gamma}H_2$ 1.37, 1.08 $C^{\gamma}H_3$ 0.81 $C^{\delta}H_3$ 0.75	7.8
Cys27	9.00	5.64	3.72, 3.02	54.1		
Ala28	10.34	4.63	1.38	51.8		10.2
Hyp29	--	4.54	2.32, 1.82	61.9	$C^{\gamma}H$ 4.50 $C^{\delta}H_2$ 3.80, 3.66	--
Ser30	8.58	4.28	3.98, 3.76	58.4		7.6
Thr31	7.98	4.23	4.23	62.3	$C^{\gamma}H_3$ 1.16	8.8
Asn32	8.26	4.58	2.78, 2.59	53.6	$N^{\gamma}H_2$ 7.40, 6.76	9.0
Trp33	7.90	4.65	3.26	57.7	C(2)H 7.23 C(4)H 7.61 C(5)H 7.15 C(7)H 7.48 NH 10.08	8.7
Ile34	7.64	3.98	1.70	62.2	$C^{\gamma}H_2$ 0.92, 0.73 $C^{\gamma}H_3$ 1.48 $C^{\delta}H_3$ 1.16	7.9
Leu35	7.58	4.68	1.48	52.6	$C^{\delta}H_3$ 0.88	7.7
Pro36	--	4.41	2.28, 1.91	63.7	$C^{\gamma}H$ 2.02 $C^{\delta}H_2$ 3.77, 3.63	--
Gly37	8.40	4.15, 3.84		45.5		
Cys38	8.31	4.47	2.29, 2.07	??		6.4
Ser39	8.47	4.29	3.96, 3.75	??		
Thr40	8.15	4.40	4.34	62.1	$C^{\gamma}H_3$ 1.24	7.0
Ser41	8.24	4.43	3.89, 3.83	58.6		6.8
Ser42	8.26	4.40	3.75	59.2		7.3
Phe43	8.08	4.52	2.98, 2.91	58.1	C(2,6)H 7.13 C(3,5)H 7.30	
Phe44	7.95	4.56	3.07, 2.94	57.7	C(2,6)H 7.20 C(3,5)H 7.33	7.3
Lys45	8.04	4.28	1.77, 1.66	56.4	$C^{\gamma}H_2$ 1.35 $C^{\varepsilon}H_2$ 2.97	6.7
Ile46	7.73	4.03	1.79	63.2	$C^{\gamma}H_2$ 1.44, 1.14 $C^{\gamma}H_3$ 0.89 $C^{\delta}H_3$ 0.88	7.8

Table S2. Chemical shifts and $^{3}J_{HNHA}$ of ι-RXIA in 95% H_2O/5% $^{2}H_2O$ at pH 5.9 and 298 K. Where there is no entry for $^{3}J_{HNHA}$, the peak intensity was weak in the DQF-COSY spectrum and the derived coupling constant was not reliable.

Residue	HN	$C^{\alpha}H$	$C^{\beta}H$	$^{15}N(H)$	Other	$^{3}J_{HNH\alpha}$
Gly1	--	4.02, 3.93				--
Hyp2	--	4.50	2.04, 1.99			--
Ser3	8.58	4.39	3.80	117.6		7.7
Phe4	8.22	4.73	3.17, 3.03	121.4	C(2,6)H 7.26, C(3,5)H 7.38	7.3
Cys5	7.98	4.52	3.05, 2.80	118.7		6.5
Lys6	8.69	4.34	2.14, 1.75	119.5	$C^{\gamma}H$ 1.56, 1.46 $C^{\delta}H_2$ 1.60 $C^{\varepsilon}H_2$ 2.99	6.0
Ala7	8.43	4.07	1.45	126.3		6.9
Asp8	8.16	4.10	2.73, 2.54	117.6		7.3
Glu9	9.21	3.80	2.30, 2.27	111.9	$C^{\gamma}H_2$ 2.57	
Lys10	7.50	4.70	2.04, 1.76	119.3	$C^{\gamma}H$ 1.56, 1.48 $C^{\varepsilon}H_2$ 3.05	6.5
Hyp11	--	4.61	2.39, 2.00		$C^{\gamma}H$ 5.18 $C^{\delta}H2$ 3.89, 3.80	--
Cys12	8.29	4.80	3.16, 3.10	124.3		7.6
Glu13	8.77	4.16	1.62, 1.44	117.6	$C^{\gamma}H2$ 1.95, 1.75	7.8
Tyr14	7.91	4.82	3.39, 2.55	117.9	C(2, 6)H 7.23 C(3, 5)H 6.80	7.1
His15	8.52	4.50	3.31,3.09	122.2	C(2)H 7.79 C(4)H 7.14	
Ala16	8.38	4.21	1.46	117.2		7.3
Asp17	7.88	4.45	3.19, 2.71	116.1		7.0
Cys18	7.93	4.89	3.11, 2.51	117.3		9.3
Cys19	9.23	4.50	2.96, 2.53	121.7		6.9
Asn20	8.58	5.02	2.72, 2.38	118.6	$N^{\gamma}H_2$ 9.07, 6.59	9.7
Cys21	8.12	5.23	3.06, 2.60	118.8		8.9
Cys22	12.03	5.05	2.76, 2.57			
Leu23	8.76	4.69	1.60	131.4	$C^{\gamma}H$ 1.45 $C^{\delta}H_3$ 0.82	10.0
Ser24	8.92	3.88	4.09	120.2		8.3
Gly25	7.59	4.08, 3.78		103.4		--
Ile26	7.52	4.73	1.61	121.3	$C^{\gamma}H_2$ 1.37, 1.07 $C^{\gamma}H_3$ 0.81 $C^{\delta}H_3$ 0.75	7.6
Cys27	8.97	5.61	3.70, 3.00	125.5		

Residue	HN	$C^{\alpha}H$	$C^{\beta}H$	$^{15}N(H)$	Other	$^{3}J_{HNH\alpha}$
Ala28	10.34	4.62	1.38	130.0		10.5
Hyp29	--	4.49	2.29, 1.80		$C^{\delta}H_2$ 3.79, 3.64	--
Ser30	8.47	4.30	3.89, 3.76	118.6		7.1
Thr31	8.02	4.30	4.26	115.7	$C^{\gamma}H_3$ 1.15	8.9
Asn32	8.27	4.58	2.79, 2.61	119.2	$N^{\gamma}H_2$ 7.41, 6.78	9.2
Trp33	7.94	4.62	3.26	120.0	C(2)H 7.22 C(4)H C(5)H 7.15 C(7)H 7.48 NH 10.07	8.8
Ile34	7.63	4.00	1.73	119.7	$C^{\gamma}H_2$ 0.98, 0.76 $C^{\gamma}H_3$ 1.22 $C^{\delta}H_3$ 1.16	7.6
Leu35	7.71	4.71	1.47	124.3	$C^{\delta}H_3$ 0.89	7.4
Pro36	--	4.41	2.29, 1.92		$C^{\delta}H_2$ 3.77, 3.63	--
Gly37	8.43	4.15, 3.86		108.9		--
Cys38	8.13	4.43	2.26, 2.03	118.4		6.9
Ser39	8.36	4.52	3.73	119.0		
Thr40	8.26	4.61	4.33	114.6	$C^{\gamma}H_3$ 1.23	7.9
Ser41	8.46	4.43	3.83	117.6		7.8
Ser42	8.25	4.75	3.73	117.7		6.5
Phe43	8.00	4.50	3.00, 2.84	120.0	C(3, 5)H 7.31 C(2, 6)H 7.11	
Phe44	7.90	4.60	3.01, 2.88	122.0	C(3, 5)H 7.34 C(2, 6)H 7.20	8.0
Lys45	8.26	4.28	1.73, 1.56	116.1	$C^{\gamma}H$ 1.35 $C^{\varepsilon}H_2$ 2.97	8.3
Ile46	7.83	4.08	1.81	127.1	$C^{\gamma}H_2$ 1.08 $C^{\gamma}H_3$ 0.86	7.9

Figure S1. NOE build-up rates in ι-RXIA[L-Phe44] monitored from a number of cross peaks at 25 °C, pH 5.9 and 600 MHz.

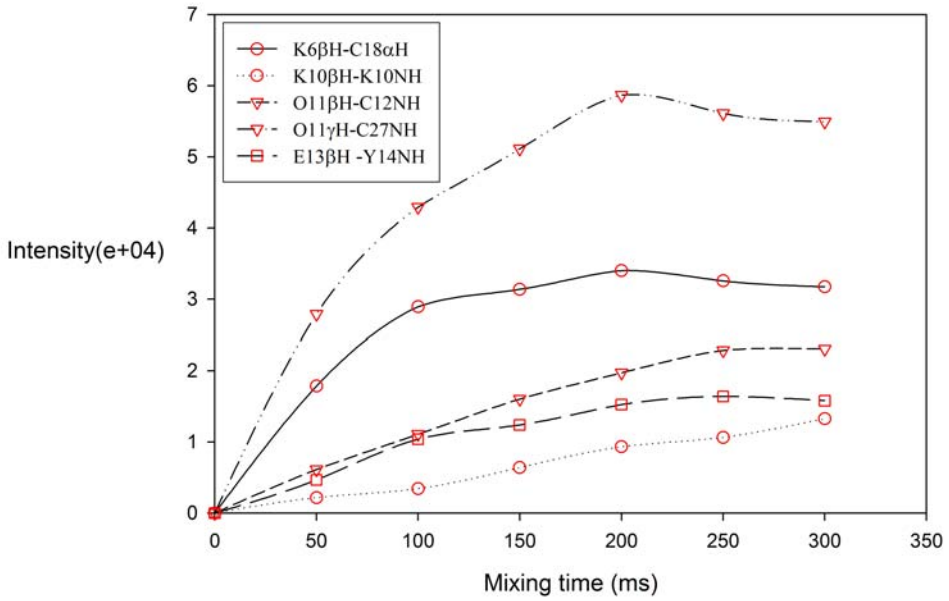

Figure S2. Amide and aromatic regions of one-dimensional ^{1}H NMR spectra of ι-RXIA[L-Phe44] at different pH values. A, B, C correspond to pH 2.8, 5.9, and 6.9, respectively.

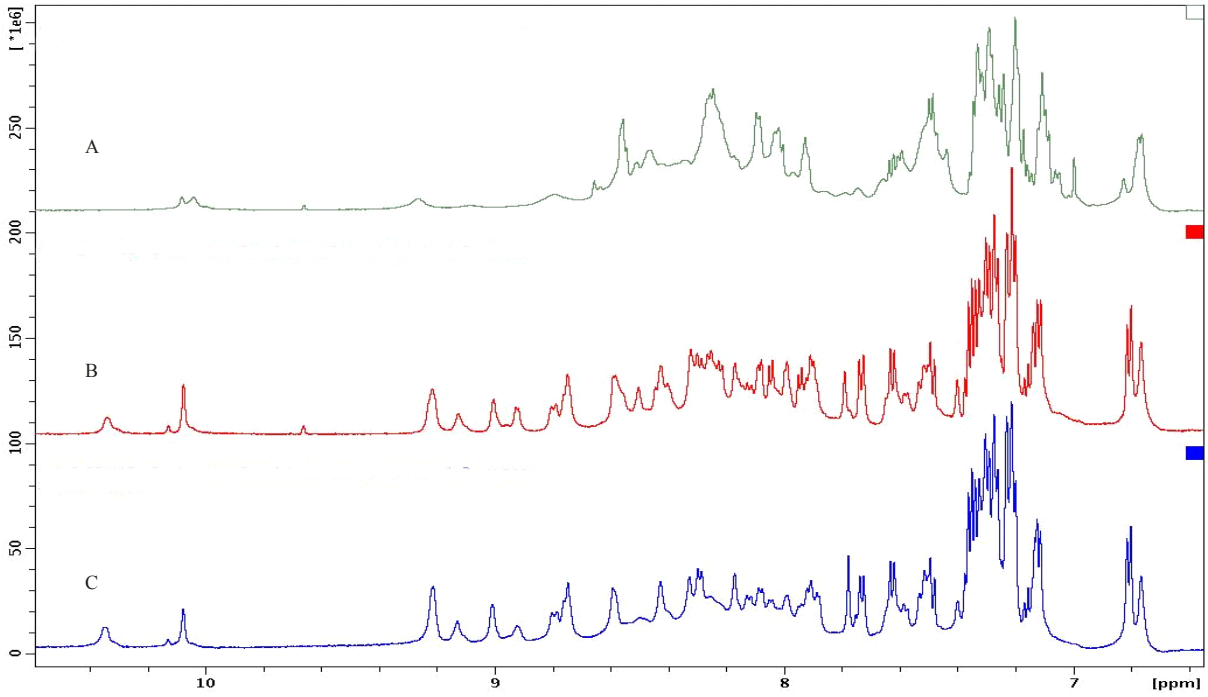

Figure S3. Plots as a function of residue number of (A) number of NOE constraints used in the final round of structure refinement of ι-RXIA[L-Phe44], and (B) to (D) the angular order parameters of the backbone and side-chain dihedral angles. All parameters were calculated from the final refined structures. Corresponding values for ι-RXIA are shown in (E) to (H). In (A, E), black, red, green, and orange colors denote intra, sequential, medium-range, and long-range NOEs, respectively. Each constraint is counted twice except for intra-residue constraints. In (B, F), there are blanks for Gly1, Hyp2, Hyp11, Hyp29, Pro36.

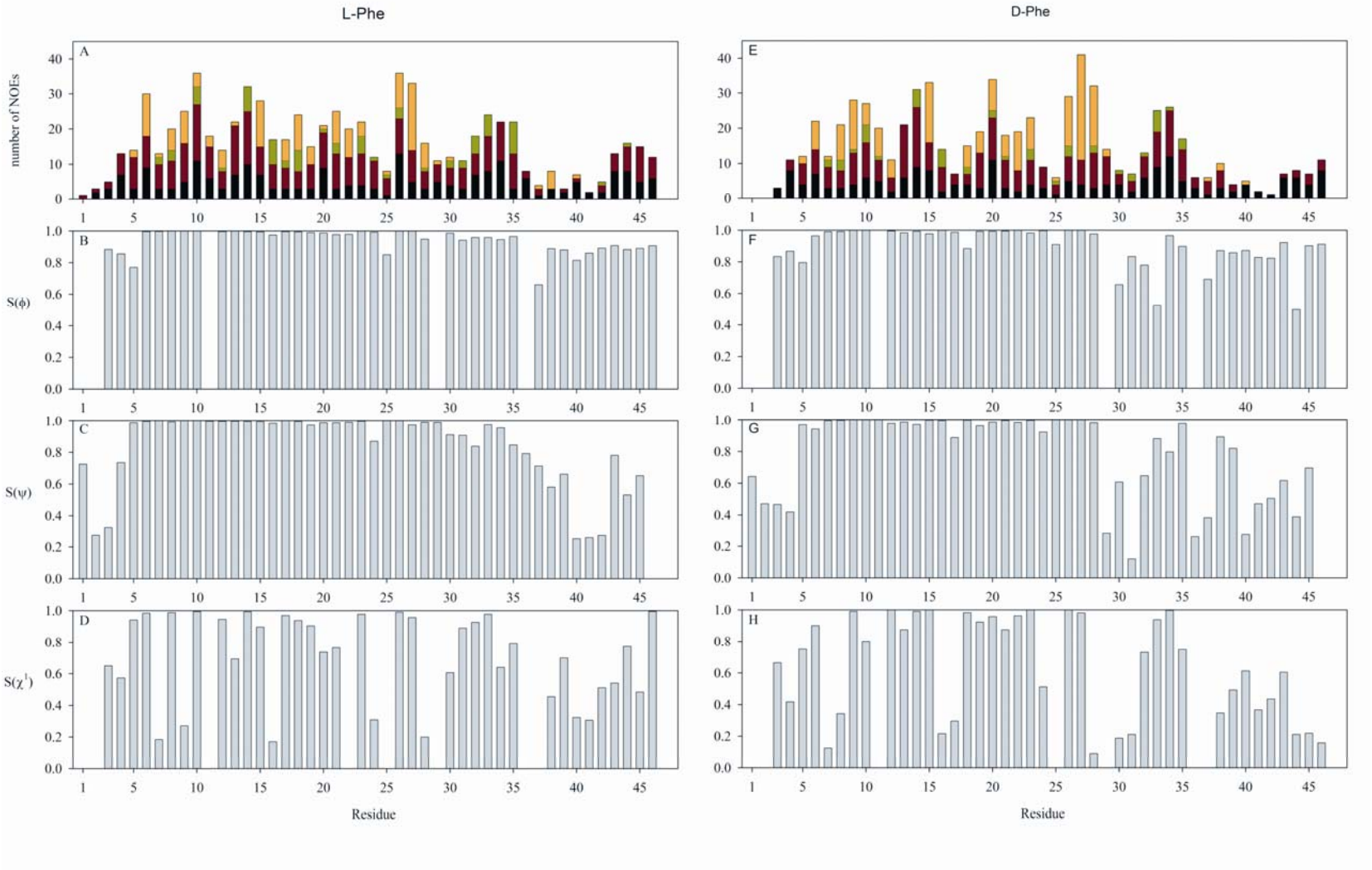

Table S3. Z-scores from Dali for comparisons among ι-RXIA[L-Phe44], J-ACTX-Hv1c, robustoxin, versutoxin and ω-agatoxin IVB, over residues 1-46 of ι-RXIA.

	ω-Aga IVB (1AGG)	ω-Aga IVB (1OMA)	Robustoxin	Versutoxin	J-ACTX-Hv1c
ι-RXIA[L-Phe44]	0.6	0.5	0.2	0.6	-- *
ω-Aga IVB (1AGG)		3.2	2.2	2.3	3.1
ω-Aga IVB (1OMA)			0.8	1.7	2.8
Robustoxin				3.5	2.1
Versutoxin					3.8

* Z-score for r11a vs J-ACTX-Hv1c could not be obtained because "No significant similarities were detected. Possible reasons: empty input or dissimilar structures"

Figure S4. Superimposition of the structures of ι-RXIA[L-Phe44] (black ribbon with blue β-sheet with (A) ω-agatoxin IVB (grey ribbon with red β-sheet), (B) robustoxin, (C) versutoxin, (D) J-ACTX-Hv1c. The backbone heavy atoms of residues in the β-sheet and the C^{α} and C^{β} atoms of the half-cystines of the ICK motif were used for superimposition.

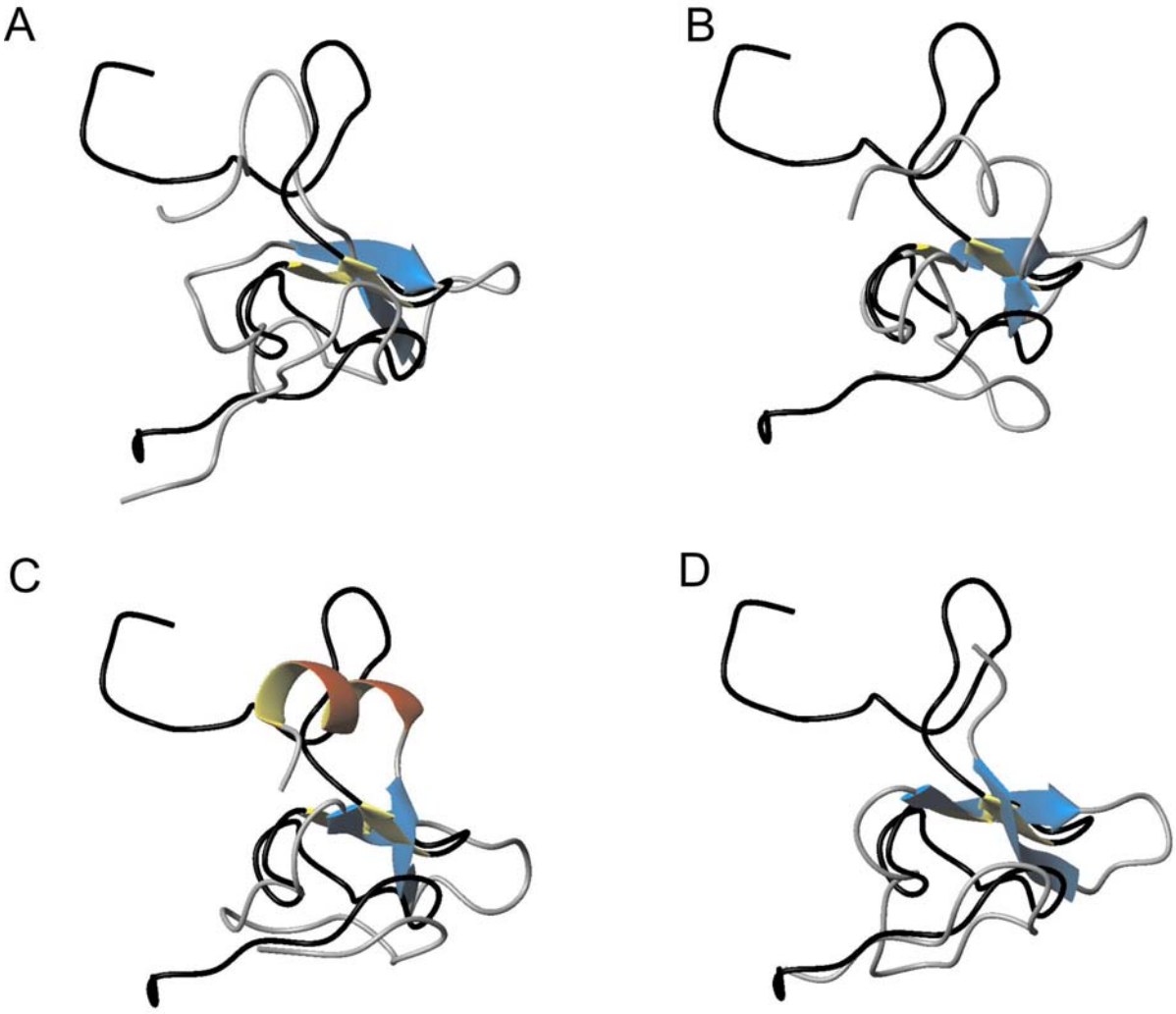

RMSD values over the residues and atoms indicated below (disulfide bond atoms are highlighted in green and β-sheet atoms in cyan):

1. ι-RXIA[L-Phe44](1) vs J-ACTX-Hv1c(2)
#1:5,12,18,19,22,27@CA,CB #2:3,10,16,17,22,33@CA,CB
#1:21,22,27,28@N,CA,C #2:21,22,32,33@N,CA,C
RMSD 1.32Å

2. ι-RXIA[L-Phe44](1) vs ω-agatoxin(2) (RCSB 1OMA)
#1:5,12,18,19,22,27@CA,CB #2:4,12,19,20,25,36@CA,CB
#1:21,22,27,28@N,CA,C #2:25,26,35,36@N,CA,C
RMSD 3.00 Å

3. ι-RXIA[L-Phe44](1) vs ω-agatoxin(2) (RCSB 1AGG)
#1:5,12,18,19,22,27@CA,CB #2:4,12,19,20,25,36@CA,CB
#1:21,22,27,28@N,CA,C #2:25,26,35,36@N,CA,C
RMSD 2.80 Å

4. ι-RXIA[L-Phe44](1) vs robustoxin(2)
#1:5,12,18,19,22,27@CA,CB #2:1,15,8,20,16,42@CA,CB
#1:21,22,28@N,CA,C #2:19,20,32@N,CA,C
RMSD 3.72 Å

5. ι-RXIA[L-Phe44](1) vs versutoxin(2)
#1:5,12,18,19,22,27@CA,CB #2:1,15,8,20,16,42@CA,CB
#1:21,22,28@N,CA,C #2:19,20,32@N,CA,C
RMSD 3.39 Å

Figure S5. Plots as a function of residue number of the mean pairwise RMSD values across the final families of 20 structures for (A) ι-RXIA[L-Phe44] and (B) ι-RXIA, in each case superimposed over the backbone heavy atoms (N, C^{α}, C) of residues 5-30. (C) Corresponding plot for superposition of all 40 structures (20 structures for ι-RXIA[L-Phe44] and 20 for ι-RXIA).